February 2006 Volume 2 Issue 1

Trade Science Inc.

Materials Science

An Indian Journal

Full Paper

MSAIJ, 2(1), 2006 [24-32]

Glass-Transition Behavior And Pre-Crystallization Kinetics Of The Semiconducting $Sb_{9.1}Te_{20.1}Se_{70.8}$ Alloy Using The Non-Isothermal Differential Scanning Calorimetry (DSC) Technique

A.A.Joraid
Physics Department,
Taibah University,
Madinah (SAUDI ARABIA)
Tel: 00966-48226462; fax: 00966-48233727.
E-mail: aaljoraid@kau.edu.sa

Received: 13th January, 2006
Accepted: 4th March, 2006

Web Publication Date : 4th April, 2006

ABSTRACT

The chalcogenide glass system $Sb_{9.1}Te_{20.1}Se_{70.8}$ was studied by differential scanning calorimetry (DSC) under non-isothermal conditions. The analyses were focused on the endothermic peaks of the DSC curves. The models used for calculation of the crystallization kinetics from the exothermic peaks were applied to obtain the pre-crystallization kinetics. A comparison of different methods of analysis is presented. The effect of heating rate on the activation energy of glass transition E_g and the Avrami index n are reported.

KEYWORDS

Pre-crystallization kinetics;
Thermal analysis;
DSC;
Heating rate.

INTRODUCTION

The study of the crystallization kinetics of amorphous materials has been widely discussed in the literature[1–6]. Different methods have been proposed for obtaining crystallization kinetics from the exothermic peaks of differential scanning calorimetry.

The pre-crystallization kinetics is the parameters that control the amorphous-glass reaction[7]. Analyses of endothermic (glass-transition) peaks could be made in the same way as those made of the exothermic (crystallization) peaks to obtain the pre-crystallization kinetics, but only a few studies have been performed on pre-crystallization kinetics[7,8]. In the present work, the pre-crystallization kinetics process was investigated under non-isothermal conditions for the chalcogenide glass $Sb_{9.1}Te_{20.1}Se_{70.8}$.

Theoretical basis

The theoretical basis for interpreting DSC data is provided by the classical Johnson–Mehl–Avrami (JMA) model[9-11], in which the crystallized fraction χ can be described as a function of time *t* according to the formula

$$\chi(t) = 1 - \exp\left[-(Kt)^n\right] \quad (1)$$

Here *K* is defined as the effective overall reaction rate, which is usually assigned by an Arrhenian temperature dependence[12]:

$$K = K_0 \exp(-E_c/RT) \quad (2)$$

Where R is the universal gas constant, E_c is the effective activation energy describing the overall crystallization process and K_0 is the frequency factor, which describes the rate constant.

Over a limited range of temperatures the nucleation frequency per unit volume I_v and the crystal growth rate *u* can be expressed according to[1,5]

$$I_\mathrm{v} \approx (I_\mathrm{v})_0 \exp\left(-\frac{E_\mathrm{N}}{RT}\right) \quad (3)$$

and

$$u_\mathrm{v} \approx u_0 \exp\left(-\frac{E_\mathrm{G}}{RT}\right) \quad (4)$$

where E_N and E_G are the effective activation energies for nucleation and growth, respectively.

The overall effective activation energy for crystallization is expressed according to[1,5]

$$E = \frac{E_\mathrm{N} + mE_\mathrm{G}}{n} \quad (5)$$

where *m* is an integer or non-integer, depending on the mechanism of growth, and *n* is a numerical factor depending on the nucleation processes. When $I_v = 0$, then $n=m+1$; and when $I_v \neq 0$, then $n=m$[1,12].

Various theoretical methods have been suggested for understanding the crystallization process using non-isothermal DSC data. It is therefore interesting to use these theoretical methods for studying the pre-crystallization process. So, analyses will be made on the endothermic (glass-transition) peaks in the same way as those made on the exothermic (crystallization) peaks to obtain the pre-crystallization kinetics. An outline of these methods is described as follows.

(i) To evaluate the activation energy of glass transition E_g the useful Kissinger's relation is commonly used, which is given by[13]

$$\ln\left(\frac{\alpha}{T_\mathrm{b}^2}\right) = \mathrm{constant} - \frac{E_\mathrm{g}}{RT_\mathrm{b}} \quad (6)$$

where T_b is the peak temperature of pre-crystallization and α is the heating rate.

Kissinger's equation can be written in a simplified form[12] as

$$\ln\alpha = \mathrm{constant} - \frac{E_\mathrm{g}}{RT_\mathrm{b}} \quad (7)$$

(ii) The value of E_g is also calculated using the variation-of-onset crystallization temperature T_o with heating rate α according to the relation given by Augis and Bennett[14]:

$$\ln\left(\frac{\alpha}{T_\mathrm{b} - T_\mathrm{o}}\right) \cong \ln K_0 - \frac{E_\mathrm{g}}{RT_\mathrm{b}} \quad (8)$$

(iii) Matusita *et al.*[15] suggested a method specifically for non-isothermal experiments. The volume fraction of crystallites χ precipitated in a glass heated at constant rate α can be related to the activation energy of glass transition *Eg* through the relation

$$\ln\left[-\ln(1-\chi)\right] = -n\ln\alpha - 1.052\frac{mE_\mathrm{g}}{RT} + \mathrm{constant} \quad (9)$$

If the crystallization fraction χ is determined at a fixed temperature, at different heating rates, then the Avrami exponent *n* can be obtained from the slope of the following equation[16]:

$$\left.\frac{\mathrm{d}\{\ln[-\ln(1-\chi)]\}}{\mathrm{d}(\ln\alpha)}\right|_\mathrm{T} = -n \quad (10)$$

For a quenched glass containing no nuclei, then $n=m+1$, and for a glass that has sufficiently large nuclei before the DSC experiment, $n=m$[15]. In this work the values of the indices *n* and *m* are considered to be equal because the amorphous-glass reaction occurs in one step[7].

(iv) The activation energy of glass transition *Eg* can be determined at constant χ from the slope of the Kissinger-Akahira-Sunose method (or the generalized Kissinger method)[13-17] as

$$\left.\frac{\mathrm{d}\left[\ln\left(\alpha/T^2\right)\right]}{\mathrm{d}\left(1/T\right)}\right|_{\chi}=\frac{E_g}{R} \tag{11}$$

(v) The fifth method that we used to evaluate E_g was using the rate isoconversion method derived by Friedman[17,18] as

$$\ln\left(\frac{\mathrm{d}\chi}{\mathrm{d}t}\right)=-\frac{E_g}{RT_f}+\text{constant} \tag{12}$$

where $(\mathrm{d}\chi/\mathrm{d}t)$ is the transformation rate, T_f the temperature at any fixed stage. E_g can be obtained from the slope of plots of $\ln(\mathrm{d}\chi/\mathrm{d}t)$ versus $1/T_f$.

(vi) The sixth method that we used to evaluate E_g was using the newly derived equation introduced by Starink[17] as:

$$\ln\frac{\alpha}{T_f^{1.92}}=-1.0008\frac{E}{RT_f}+\text{constant} \tag{13}$$

E_g is determined from the slope of plots $\ln\left(\alpha/T_f^{1.92}\right)$ versus $1/T_f$.

(vii) The final method that we used to evaluate E_g was using the JMA relation directly (Eqs. 1 and 2). It should be noted, however, that Eq.(1) strictly applies only to isothermal experiments[1]. On the other hand, Eq.(1) has been used to evaluate the crystallization kinetics for non-isothermal conditions[19]:

$$K=\left(1/t\right)\left[-\ln\left(1-\chi\right)\right]^{1/n} \tag{14}$$

Taking the logarithm of Eq. (2) gives

$$\ln K=\ln K_0-E_c/RT \tag{15}$$

It is possible to use Eqs. (14) and (15) to calculate the pre-crystallization kinetics, and the value of *n* that corresponds to each heating rate can be obtained from Eq. (10).

EXPERIMENTAL TECHNIQUE

Glassy alloy of $Sb_{9.1}Te_{20.1}Se_{70.8}$ was prepared by the quenching technique. High-purity materials (99.999%) were weighed according to their atomic percentages and were sealed in quartz ampoules under a vacuum of 10^{-4} Torr. The contents were heated inside a furnace at a maximum temperature of 950 K for 24 h. To make the melting homogeneous, the ampoules were shaken frequently. The ampoules were quenched in ice water to obtain the material in a glassy state. The glassy nature of the alloys was examined by scanning electron microscope-EDX using Shimadzu Superscan SSX-550 apparatus.

Thermal behavior was investigated using a Shimadzu DSC-60 apparatus with an accuracy of ±0.1K, under dry nitrogen supplied at a rate of 35 ml min^{-1}. Typically, 3 mg of the sample in powder form was sealed in standard aluminum pans and heated at different rates, ranging from 2 to 80 K min^{-1}. To minimize the temperature gradients the samples were granulated to form uniformly fine powder and spread as thinly as possible on the bottom of the sample pans, and the weight of sample was kept very low. Temperature and enthalpy calibrations were checked with indium (T_m=156.6°C, ΔH_m=28.55 J g^{-1}) as the standard material supplied by Shimadzu.

RESULTS AND DISCUSSION

Figure 1 shows a typical DSC thermogram for the chalcogenide $Sb_{9.1}Te_{20.1}Se_{70.8}$ alloy heated at a rate of 20 K min^{-1}. Similar thermograms were obtained for other heating rates. The circled part shows the area of interest. The values associated with the four characteristic temperatures - the on-set temperature T_o, the glass transition of crystallization temperature T_g, the peak of pre-crystallization (endothermic peak) temperature T_b and the temperature T_{final} - where the glassy state was completed are shown on figure 1.

Figure 2 shows the variation of the endothermic peaks with temperature. The area under the DSC curve is directly proportional to the total amount of alloy crystallized, and the plot of this area against heating rate is shown in figure 3.

It is easily seen that the peak temperature for pre-crystallization T_b increased with increasing heating rate. Figure 4 shows the variation of T_b against heating rate α. As shown on the figure, the experimental data fit two different curve types: exponential for low heating rate ($2 \le \alpha \le 25$ K min^{-1}) and linear for high heating rate ($2 \le \alpha \le 80$ K min^{-1}), with a transition point at about $\alpha\approx26.3$ K min^{-1}.

The fraction χ transformed into the glassy state at any temperature T is given as $\chi=A_T/A$, where A

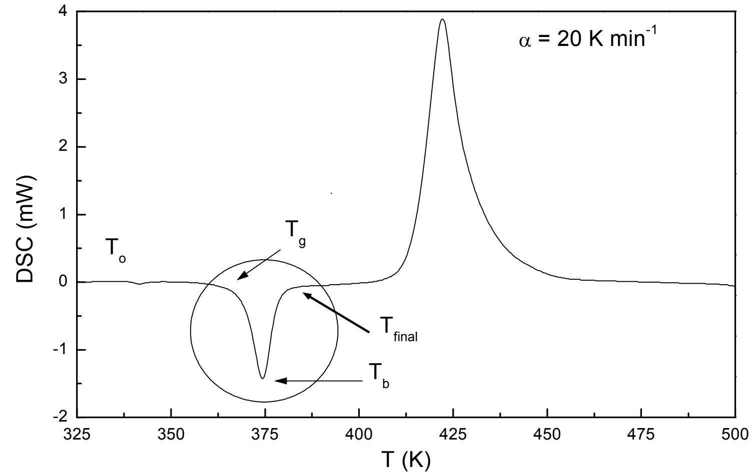

Figure 1: A typical DSC thermogram for the chalcogenide $Sb_{9.1}Te_{20.1}Se_{70.8}$ alloy heated at rate of 20 K min^{-1}. See text for details.

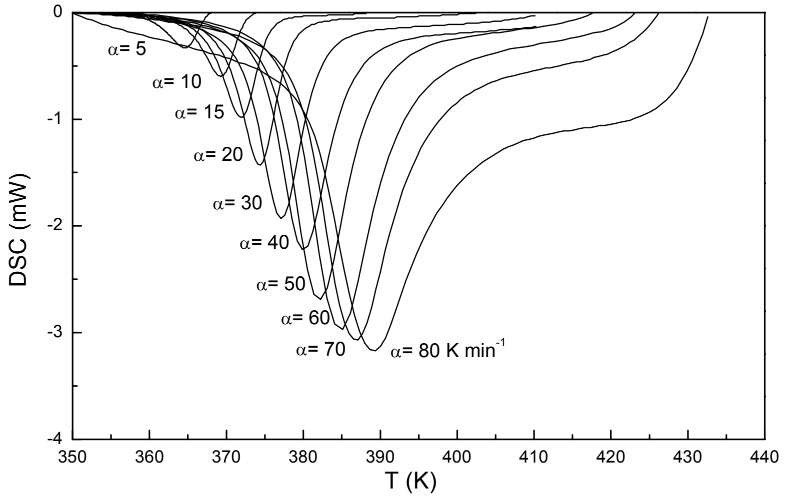

Figure 2: The variation of the endothermic peaks with temperature.

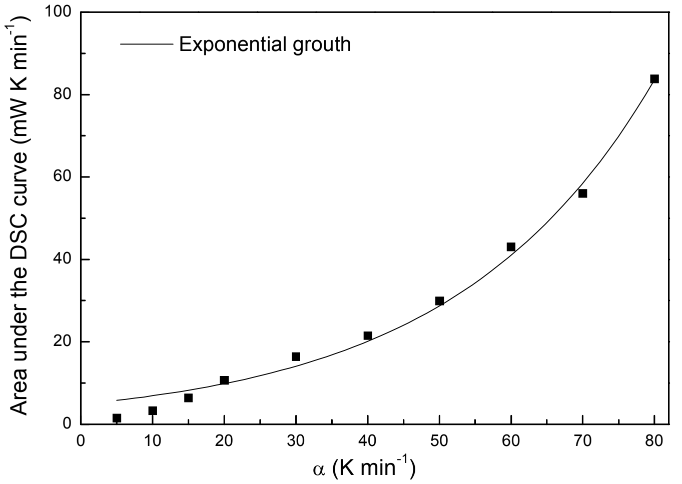

Figure 3: The variation of the area under the endothermic peaks with heating rate.

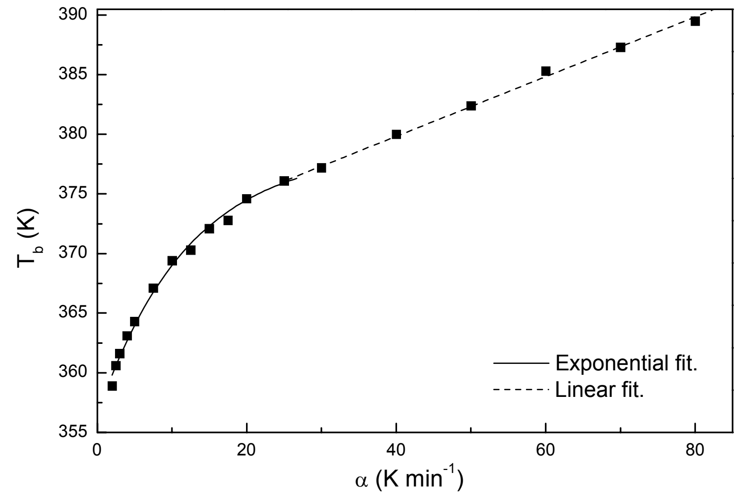

Figure 4: The variation of the peak temperature for pre-crystallization T_b with increasing heating rate.

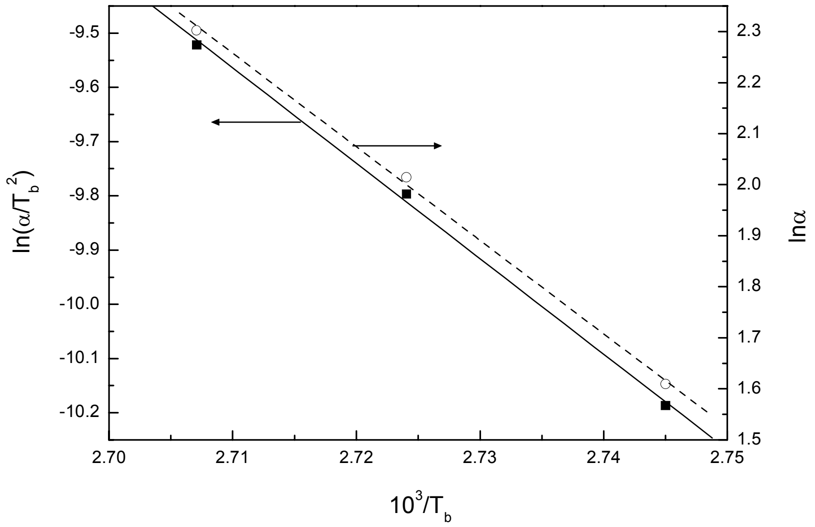

Figure 5: The variation of ln (α/T_b^2) and ln α against $10^3/T_b$ for three adjacent heating rates of α=5, 7.5, and 10 K min^{-1}.

is the total area of the endothermic peak between the glass transition temperature T_g and the final temperature of the glassy state T_{final}.

According to Kissinger's formula (Eqs. 6 and 7) plotting of $\ln\left(\alpha/T_b^2\right)$ and ln α versus $10^3/T_b$, for each three adjacent point make it possible to evaluate the variation of E_g with heating rate α=3-70 K min^{-1}. Figure 5 shows the variation of $\ln\left(\alpha/T_b^2\right)$ and ln α against $10^3/T_b$ for three adjacent heating rates of α=5,7.5, and 10 K min^{-1}. However, the variation of the glass transition energy, E_g, with heating rate, α, obtained from (Eqs. 6 and 7) will be shown later in figure 11.

From the slope of the linear fit of ln(α/T_b-T_o) against $10^3/T_b$ as shown in Figure 6 for three adjacent heating rates of α=5,7.5, and 10 K min^{-1} the value of the activation energy of glass transition E_g was obtained for heating rate of α=3-70 K min^{-1} and shown in figure 11 also.

The kinetics of crystallization were obtained using a method specifically suggested for non-isothermal conditions (Eq. 9). The plot of ln[-ln(1-χ)] against $10^3/T$ is shown in Figure 7.

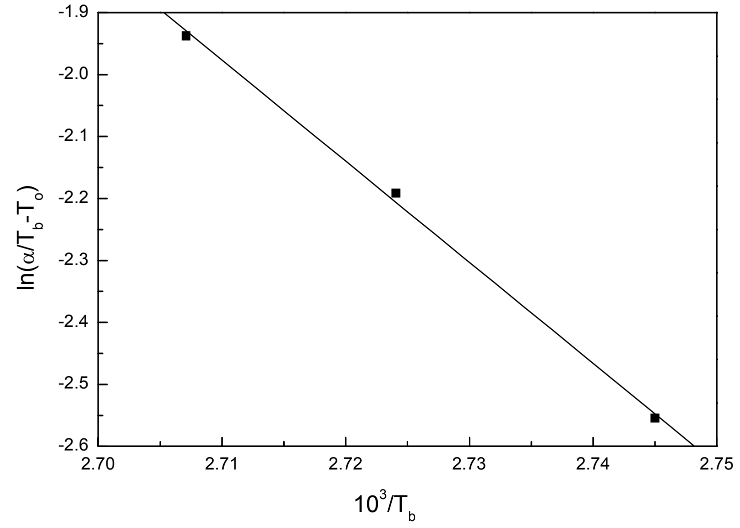

Figure 6: The variation of ln (α/T_b-T_o) against $10^3/T_b$ for three adjacent heating rates of a=5, 7.5, and 10 K min^{-1}.

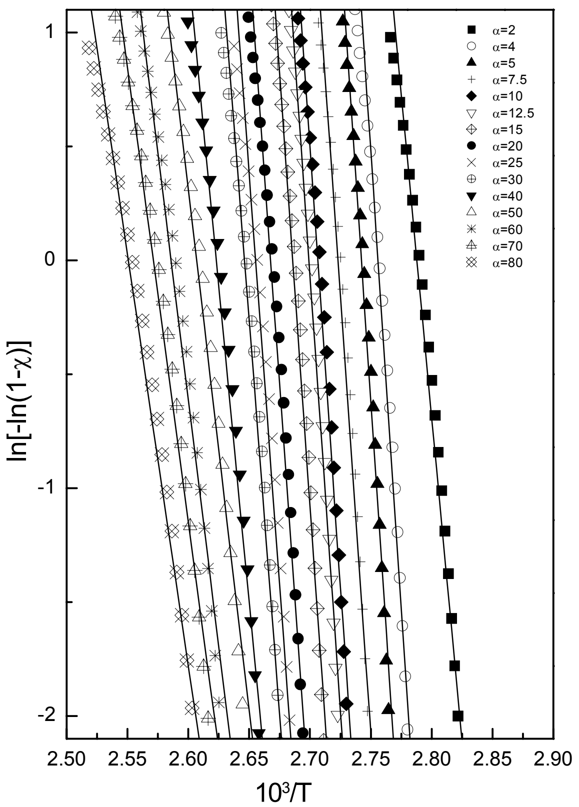

Figure 7: The plot of ln [-ln(1-χ)] against $10^3/T$ for different heating rates.

The resulting straight lines on figure 7 have slopes that vary gradually with heating rate. Using Eq. (10), the values of the Avrami exponent n were determined from the slopes of these curves.

TABLE 1

α(Kmin^{-1})	n	α(Kmin^{-1})	n	α(Kmin^{-1})	n
2	2.46	15	3.57	40	3.35
5	2.85	20	3.89	50	2.81
7.5	3.16	25	3.95	60	2.54
10	3.24	30	3.92	70	2.49

We calculated values of the Avrami exponent n as a function of heating rate α obtained from Eq. (10). The calculated values of n were not integers and showed a variation of $2.5 \le n \le 4$, with a maximum value of $n \approx 4$ at $\alpha \approx 25$ K min^{-1}. The values of n obtained are listed in TABLE 1.

The value of E_g, was obtained by using the Kissinger-Akahira-Sunose method, which also shown in Figure 11, the values obtained at χ=0.5. Figure 8 illustrates the plot of ln(α/T^2) versus (10^3/T) at three constant values of the crystallization fraction χ at three adjacent heating rate of α=5,7.5, and 10 K min^{-1}.

The values of E_g were obtained form Friedman's method Eq. (12) by using the experimental data T_b and $(d\chi/dt)|_b$ for χ=0.5. The variation of $d\chi/dt$ versus T is shown in figure 8. Figure 9 shows the variation of ln($d\chi/dt$) versus $10^3/T$.

We used to evaluate E_g the newly derived equation by Starink Eq. (13). Figure 9 shows the variation of $\ln\left(\alpha/T_b^{1.92}\right)$ against $10^3/T$. Starink reported[17]

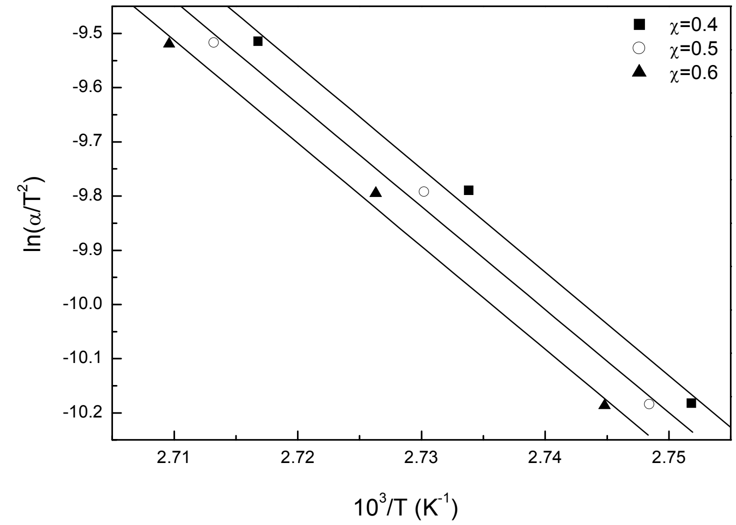

Figure 8: The plot of ln (α/T^2) versus $10^3/T$ for three adjacent heating rates of a=5, 7.5, and 10 K min^{-1} at constant χ.

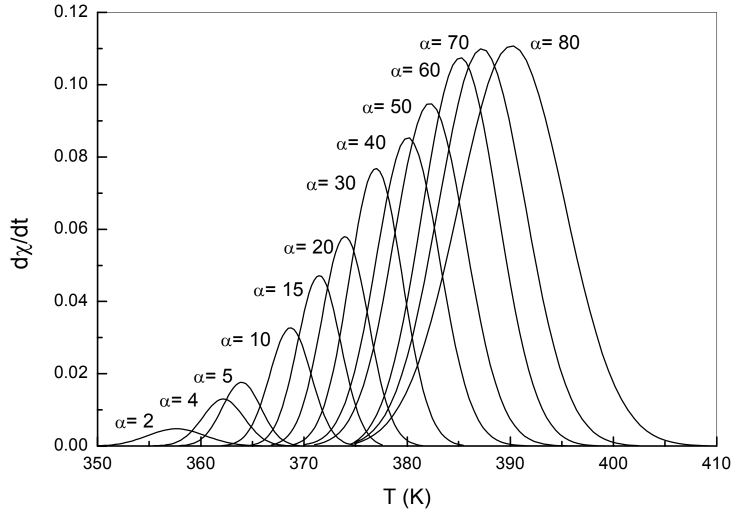

Figure 9: The variation of $d\chi/dt$ versus T for different heating rates.

that, the most accurate method and the nearest to the exact value is Starink's model Eq. (13).

However, Figure 11 shows the values of E_g obtained from the methods discussed above. It is evident from this result that the E_g values obtained from (Eqs. 6, 7, 8, 11, and 13) are in a very good agreement. In addition, Figure 11 shows the values of E_g obtained directly from the JMA equation (Eqs. 14 and 15), with the value of *n* obtained from Eq. (10). It is unambiguous that the values of E_g determined by the JMA equation directly in non-isothermal pre-crystallization agree somewhat with those obtained from the model of Matusita *et al.*[15], in particular at very high heating rate $\alpha>70$ Kmin^{-1}. Joraid reported[20] that, JMA model shows a reasonable agreement with the experimental results to describe the crystallization process for the same system of chalcogenide glass, but at high heating rates.

So, this indicates that the changing of activation energy of glass transition as shown in figure 11 means that the assumptions for all the analysis methods are not met. The Fiedman method on the one hand and the Kissinger and Starink like methods on the other hand, while Matusita method forms a third group.

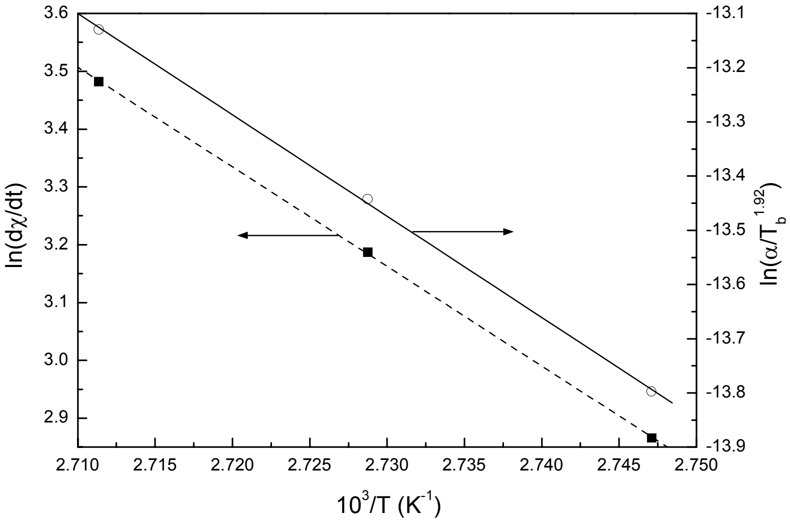

Figure 10: The plot of ln (dχ/dt) and ln($\alpha/T_b^{1.92}$) versus $10^3/T$ for three adjacent heating rates of α=5, 7.5, and 10 K min^{-1}.

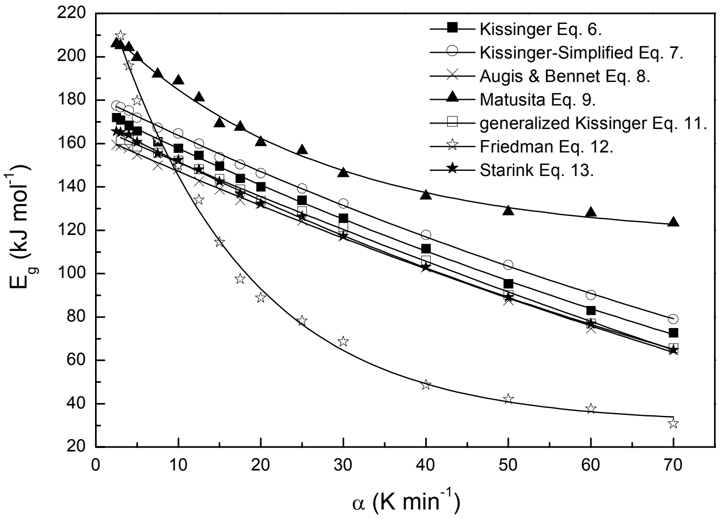

Figure 11: The plot of the glass transition crystallization energy E_g versus heating rate α for all models used.

CONCLUSION

A DSC experiment was performed to understand the process of pre-crystallization kinetics in $Sb_{9.1}Te_{20.1}Se_{70.8}$ chalcogenide glass. The value of order parameter n was found to be varied with respect to heating rates of $2.5 \leq n \leq 4$, with a maximum value of $n \approx 4$ at $\alpha \approx 25$ K min^{-1}.

The activation energy for glass transition E_g was determined using different models. The values obtained from the Kissinger, Augis and Bennett, Kissinger-Akahira-Sunose and Starink models were almost identical. Moreover, the values of E_g obtained using the models of Matusita et al. and the Friedman were to some extent different. All values measured decrease exponentially as heating rate increases.

REFERENCES

[1] H.Yannon, D.R.Uhlmann; J.Non-Cryst.Solids, **54**, 253 **(1983)**.

[2] Malek; Thermochimica Acta, **355**, 239 **(2000)**.

[3] P.L.Lopez-Alemany, J.Vazquez, P.Villares, R.Jimenez-Garay; J.Non-Cryst.Solids, **287**, 171 **(2001)**.

[4] A.A.Othman, H.H.Amer, M.A.Osman, A.Dahshan; J.Non-Cryst.Solids, **351**, 130 **(2004)**.

[5] J.Vazquez, R.Gonzalez-Palma, P.L.Lopez-Alemany, P.Villares, R.Jimenez-Garay; J.Alloys Compounds, **370**, 177 **(2004)**.

[6] N.Ziani, M.Belhadji, L.Heireche, Z.Bouchaour, M. Belbachir; Physica B, **358**, 132 **(2005)**.

[7] A.H.Moharram, M.Abu El-Oyoun; J.Phys.D.Appl. Phys., **33**, 700 **(2000)**.

[8] A.H.Moharram, A.A.Abu-sehly, M.Abu El-Oyoun, A.S.Soltan; Physica B, **324**, 344 **(2002)**.

[9] W.A.Johnson, R.F.Mehl; Trans.Am.Inst.Min.(Metal) Engs., **135**, 416 **(1939)**.

[10] M.Avrami; J.Chem.Phys., **7**, 1103 **(1939)**.

[11] M.Avrami; J.Chem.Phys., **8**, 212 **(1940)**.

[12] S.Mahadevan, A.Giridhar, A.K.Singh; J.Non-Cryst. Solids, **88**, 11 **(1986)**.

[13] H.E.Kissinger; Anal.Chem., **29**, 1702 **(1957)**.

[14] J.A.Augis, J.E.Bennett; J.Therm.Anal., **13**, 283 **(1978)**.

[15] K.Matusita, T.Komatsu, R.Yokota; J.Mater.Sci., **19**, 291 **(1984)**.

[16] T.Ozawa; Polymer, **12**, 150 **(1971)**.

[17] M.J.Starink; Thermochimica Acta, **404**, 163 **(2003)**.

[18] H.L.Friedman; J.Polym.Sci.C, **6**, 183 **(1964)**.

[19] M.Abu El-Oyoun; J.Phys.Chem.Solids, **61**, 1653 **(2000)**.

[20] A.A.Joraid; Thermochimica Acta, **436**, 78 **(2005)**.